JOURNAL OF SOLID STATE CHEMISTRY 105, 44–48 (1993)

A New Oxide Ion Conductor Family: $Bi_7(P_{1-y}V_y)O_{13}$

J. P. WIGNACOURT,* M. DRACHE, AND P. CONFLANT

Laboratoire de Cristallochimie et Physicochimie du Solide, URA CNRS 0452, ENSCL et USTL, B.P. 108, 59652 Villeneuve d'Ascq Cedex, France

Received May 21, 1992; in revised form October 1, 1992; accepted October 8, 1992

A new phase, Bi_7PO_{13}, obtained at room temperature in the Bi_2O_3–$BiPO_4$ system, has been identified as a superstructure of the δ Bi_2O_3 fcc form. Its conductivity level has been improved by a substitution of V for P, in solid solution $Bi_7(P_{1-y}V_y)O_{13}$ with $0 \leq y \leq 0.5$. Above 400°C the conduction mechanism is due to the mobility of the O^{2-} ions. The electrolyte P_{O_2} response time has been investigated vs time for successive thermal cycles. © 1993 Academic Press, Inc.

Introduction

The high temperature δ form of Bi_2O_3 is very well known for its excellent anionic conduction properties resulting from a fluorite structural type with highly disordered O^{2-} vacancies (*1*, *2*). Various chemical dopings have produced structurally related phases that maintain a $P_{O^{2-}}$ ionic conduction mechanism with a partial electronic contribution at low temperatures (*3*, *4*). In a recent reinvestigation of the Bi_2O_3–P_2O_5 system (*5*), we described a δ-sillenite-type solid solution in the range $0.10 \leq x \leq 0.143$ with $x = BiPO_4/(Bi_2O_3 + BiPO_4)$ (*6*); e.m.f. measurements have shown that an ionic–electronic mixed conduction process occurs up to 825°C, where further heating produces a multiple fluorite form ($3 \times 3 \times 3$) with transport number $t_{O^{2-}} = 1$. A partial $Bi^{3+} \rightarrow Bi^{5+}$ oxidation process has been detected for $x = 0.143$ by analytical and density measurements, and by refinement of the structure from powder X-ray diffraction data.

Two other phases, ε and σ, have been characterized in this system as superstructures of the δBi_2O_3 fcc form. At room temperature, their compositions are limited to $x = 0.25$ and $x = 0.30$, respectively. Their solid solution ranges widen with increasing temperature, with an $\varepsilon \rightarrow \sigma$ transformation occuring at 875°C.

Both forms have monoclinic unit cells, identified from single-crystal data; their common relationship with the δ-fluorite structure has been described previously (*7*).

γ, ε, and σ solid solutions show similar conductivity behavior vs temperature, the best conductor being the ε phase. In previous investigations of the M_2O–Bi_2O_3–(P_2O_5 or V_2O_5) systems (*8*, *9*), we have noted a systematically higher conductivity level in V-containing phases. This paper deals with a V doping of the P sites in the ε solid solution ($x = 0.25$).

Experimental

Compounds corresponding to the general formula $Bi_7(PO_4)_{1-y}(VO_4)_yO_9$ have been obtained by solid state reaction of Bi_2O_3, $(NH_4)_2HPO_4$, and V_2O_5 in alumina crucibles according to the scheme

$$\frac{7}{2}Bi_2O_3 + (1-y)(NH_4)_2HPO_4 + \frac{y}{2}V_2O_5 \rightarrow Bi_7(PO_4)_{1-y}(VO_4)_yO_9 + 2(1-y)NH_3 + \frac{3}{2}(1-y)H_2O,$$

where $0 < y < 1$. Initial firing at 350°C for

* To whom correspondence should be addressed.

0022-4596/93 $5.00

5 hr leads to a full decomposition of $(NH_4)_2HPO_4$; a further standard treatment is heating at 770°C for 15 hr, then 820°C for 15 hr, with an intermediate regrinding. The sample is finally air-quenched. The completeness of the reaction is routinely checked by room-temperature X-ray diffraction (Guinier–De Wolff camera); a Siemens D 5000 diffractometer has been used for intensity measurements. Thermal investigations were done using high-temperature X-ray diffractometry (HTXRD) with a Guinier–Lenné camera (heating rate 20°/hr), differential thermal analysis (D.T.A., 300°/hr), and thermogravimetric analysis (T.G.A., 120°/hr). Investigations of the electrical properties were carried out on materials sintered near 900°C and then annealed at 800°C before the measurements were run. Conductivity measurements were done by complex impedance spectroscopy (Solartron 1170) in air, in the frequency range $1–10^6$ Hz, with 1 hr stabilization for each investigated temperature, using cylindrical pellets (5 mm diameter, 3 to 4 mm thickness) with gold electrodes deposited on both flat faces.

The transport number of the ionic species O^{2-} was evaluated from the emf of the concentration cell $P_1(O_2)$/Au/sample/Au/$P_2(O_2)$ as a function of temperature. Discs of two compositions, $y = 0$ and 0.4, were used (10 mm ϕ × 10 mm). Gold grids were cold pressed onto the faces of the discs, then annealed at 900°C for 15 hr to attach them to the pellets (Fig. 1). The emf of the concentration cell was studied in the temperature range 250–800°C, with air and pure oxygen as anode and cathode gases. The reversibility of the cell was systematically controlled by exchanging these atmospheres. We used a high impedance (10^{14} Ω) voltmeter; because of the high resistivity of the investigated samples at low temperatures we started our measurements at 300°C for $Bi_7(PO_4)O_9$, and at 250°C for $Bi_7(PO_4)_{0.6}(VO_4)_{0.4}O_9$.

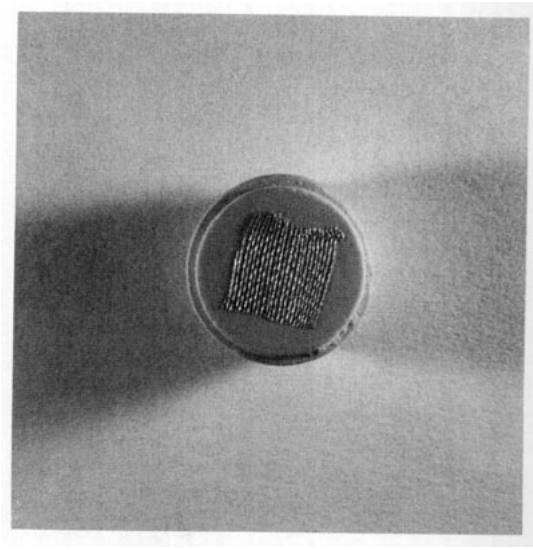

FIG. 1. Gold grid electrode on the sample for emf measurements.

Discussion

The X-ray diffraction patterns of the samples are typical of three different domains:

* for $0 \leq y \leq 0.5$, the original pattern of the ε phase is maintained, with a decrease in the diffraction angles related to the increase of y (vanadium content);

* for $0.55 \leq y \leq 1$, a different solid solution is obtained;

* a mixture of both phases is encountered in the range $0.5 < y < 0.55$.

Our previous knowledge of the lattice parameters of $Bi_7(PO_4)O_9$ ($y = 0$) led us to focus this work on the domain $0 \leq y \leq 0.5$. The lattice constants were obtained from examination of a single crystal (*7*). The powder pattern obtained from crushed crystals is exactly the same as that from corresponding powdered samples. On the basis of this unit cell, we have indexed the powder patterns throughout the solid solution domain. The 25 most intense peaks of $Bi_7(PO_4)O_9$ are described in Table I; Table II lists the refined parameters for the ε solid solution. The unit cell variation vs composition is typical for vanadium substitution for phosphorus.

TABLE I

X-RAY POWDER DIFFRACTION DATA FOR $Bi_7(PO_4)O_9$

h	k	l	d_{obs}	I/I_0 (%)
−2	0	1	9.771	1.5
−1	1	3	6.707	4.5
0	2	1	5.815	5
−4	0	2	4.902	3
−4	0	3	4.763	4
0	0	5	4.518	2.5
1	3	1	3.828	4
−5	1	3	3.706	2
1	3	−3	3.593	2.5
−5	1	0	3.496	3
0	0	7	3.230	100
−6	0	1	3.172	68.5
−6	0	5	3.117	69.5
−4	2	6	3.111	72
6	0	1	2.874	5
−5	3	2	2.803	49.5
4	2	4	2.714	3.5
6	0	−8	2.608	25
6	0	6	2.027	14.5
−10	0	3	1.946	14
9	1	1	1.938	15
8	2	−10	1.919	15.5
9	3	−6	1.896	16

The thermal properties of the ε solid solution have been studied by HTXRD and D.T.A. The $\varepsilon \rightarrow \sigma$ transition occurs at 875°C for $y = 0$, but no phase transformation was observed in the solid state for the rest of the domain ($y = 0.1$ to 0.4). We have investigated the conductivity between 350°C and 800°C. In this temperature range, the impedance plot does not provide any indication of grain boundary conductivity. On the Arrhenius plot of conductivity for the first heating, anomalies, which disappear on cooling, can be related to a progressive annealing that follows the initial quenching of the pellets. A further thermal cycle yields perfectly reproducible conductivity measurements. Figure 2 shows log σ as a function of $1/T$ during the first cooling for three different compositions in the solid solution domain ($y = 0$, 0.1, 0.4). The conductivity values range from 10^{-5} to $10^{-2}\ \Omega^{-1}\ cm^{-1}$ between 350 and 800°C, with an activation energy of approximately 0.8 e.V.

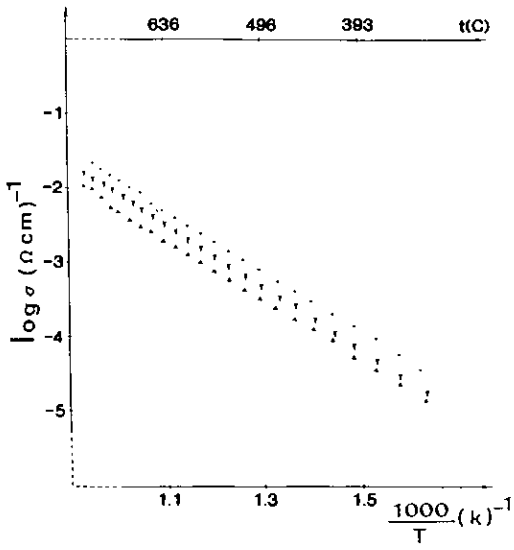

FIG. 2. Arrhenius plots of conductivity for the first cooling for $Bi_7(P_{1-y}V_y)O_{13}$ samples ($y = 0$, ▲; 0.1, ▼; 0.4, ●).

Phases with a fluorite-type structure are well known for their O^{2-} ionic conduction properties. In order to check the conduction

TABLE II

REFINED CELL PARAMETERS FOR $Bi_7(P_{1-y}V_y)O_{13}$ SOLID SOLUTION

y	a_m(Å)	b_m(Å)	c_m(Å)	β_m(°)	V_m(Å^3)
0	19.649(6)	12.031(12)	24.341(13)	111.81(3)	5342.3
0.1	19.669(5)	12.102(8)	24.371(9)	111.76(3)	5388.1
0.25	19.706(6)	12.094(6)	24.432(11)	111.97(3)	5400.4
0.40	19.775(8)	12.130(10)	24.589(13)	112.29(4)	5457.3
0.50	19.790(11)	12.159(21)	24.613(16)	112.34(5)	5477.8

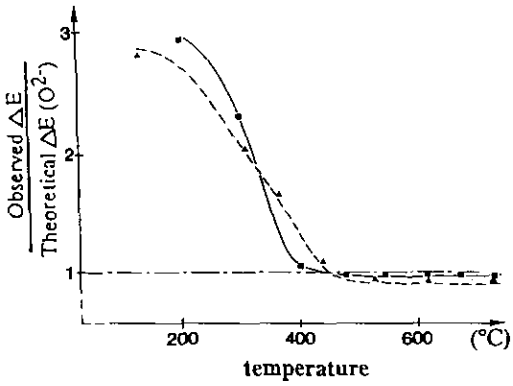

FIG. 3. Temperature dependence of observed/calculated $\Delta E(O^{2-})$ ratio of an oxygen concentration cell for $Bi_7(P_{1-y}V_y)O_{13}$ samples (y = 0, ■; 0.4, ▲).

mechanism in the ε solid solution, we made emf measurements of an oxygen concentration cell using our samples as solid electrolytes.

Figure 3 shows the dependence on temperature of the ratio (observed emf/theoretical emf) corresponding to the classical Nernst Law:

$$O_{2(gas)} + 4e^- \rightarrow 2\,O^{2-}\ (\text{electrode}). \quad (1)$$

Figure 4 presents the response time vs the temperature; both representations are provided between the selected temperature and 550°C. No further modification is noted above that temperature. Near 300°C, the voltages are about 2 or 3 times greater than the expected values, with a maximum response time. When the temperature is at least 420°C, a transport number close to 1 proves that the O^{2-} ionic conduction predominates in both samples. At 420°C the equilibrium voltage is reached in 30 min for y = 0, and 8 min for y = 0.4; for that last composition it was achieved very rapidly at 500°C (i.e., the time needed to purge the equipment). The same study has been done for the y = 0.4 sample equipped with vacuum-deposited gold electrodes; we have obtained the identical responses for a long heating–cooling cycle (10 days) 200–800–200°C, with the maximum voltage value observed during both the heating and the cooling processes. This maximum is independent of the electrolyte interface. A possible contribution from H^+ ion migration associated with absorbed H_2O can be ruled out from a thermogravimetric analysis which attests to the thermal stability of our sample in the temperature range 25–500°C. Such high values of the ratio observed emf/theoretical emf (i.e., from 2 to 4) requires the modification of the Nernst Law as already described in the literature for different types of materials and electrodes (*10*). This phenomenon is due to the replacement of the high-temperature reaction (1) by the successive slower elementary reactions

$$O_2 + 1\,e^- \rightarrow O_2^- + 1\,e^- \rightarrow (O_2)^{2-} \rightarrow 2\,O^- + 2\,e^- \rightarrow 2\,O^{2-}. \quad (2)$$

In this description, the intervening formation of the $(O_2)^{2-}$ peroxide ion has been checked by the study at various temperatures of the voltage as a function of

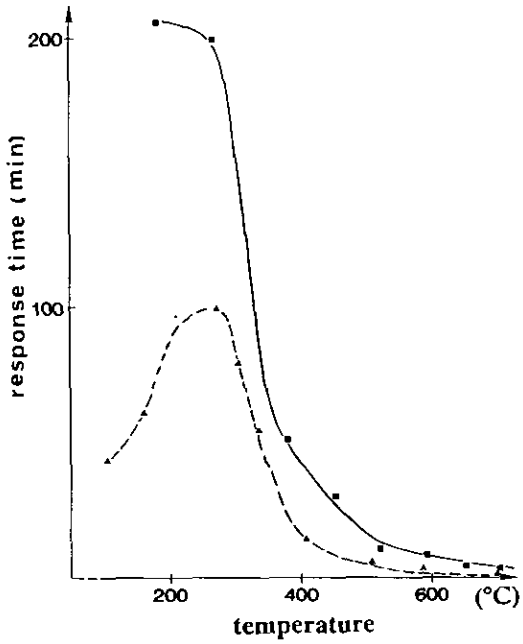

FIG. 4. Temperature dependence of the response time to P_{O_2} variation of an oxygen concentration cell for $Bi_7(P_{1-y}V_y)O_{13}$ samples (y = 0, ■; 0.4, ▲).

$\ln(P_{O_2})$. The conclusions were: (i) At high temperatures only the reaction (1) mechanism is encountered. (ii) At moderate temperatures (i.e., 300°C), two different behavior patterns are noted, depending on the P_{O_2} values: For low pressures, the usual reaction (1) is maintained. For high pressures, peroxide formation occurs according to

$$O_2 + 2\,e^- \rightarrow (O_2)^{2-}, \qquad (3)$$

as has been verified from experimental data. This reaction (3) becomes preponderant at temperatures below 200°C.

Conclusion

The ε phase, previously described in the Bi_2O_3–P_2O_5 system, has a wide stability range in the ternary Bi_2O_3–$BiPO_4$–$BiVO_4$ diagram. The corresponding materials exhibit substantial ionic conductivity above 420°C; the substitution of V for P improves the conductivity level, and the pO_2 response time is drastically shortened before vanishing at 500°C. These values remain remarkably constant for long time thermal cycles, thus making these phases attractive for technical use.

References

1. T. Takahashi, H. Iwahara, and Y. Nagai, *J. Appl. Electrochem.* **2,** 97 (1972).
2. H. A. Harwig, *Z. Anorg. Allg. Chem.* **444,** 151 (1978).
3. P. Conflant, Thesis, Lille, 1985.
4. T. Graia, P. Conflant, J. C. Boivin, and D. Thomas, *Solid State Ionics* **18–19,** 751 (1986).
5. J. P. Wignacourt, M. Drache, P. Conflant, and J. C. Boivin, *J. Chim. Phys.* **88,** 1933 (1991).
6. J. P. Wignacourt, M. Drache, P. Conflant, and J. C. Boivin, *J. Chim. Phys.* **88,** 1939, 1991.
7. T. Guédira, Thesis, Lille, 1989.
8. M. F. Debreuille-Gresse and F. Abraham, *J. Solid State Chem.* **71,** 466 (1987).
9. M. Diouri, A. Sadel, M. Zahir, M. Drache, P. Conflant, J. P. Wignacourt, and J. C. Boivin, *J. Alloys and Compounds,* **188,** 206 (1992).
10. E. Siebert, Thesis, Grenoble, 1987.